# B. Graphite Foam for Cooling Power Electronics

*Nidia C. Gallego*
*Oak Ridge National Laboratory*
*P.O. Box 2008, MS 6087, Bldg. 4508*
*Oak Ridge, TN 37831-6087*
*(865) 241-9459; fax: (865) 576-8424; e-mail: gallegonc@ornl.gov*

*Albert Shih, Steve White*
*S. M. Wu Manufacturing Research Center*
*University of Michigan*

*Anthony G. Straatman*
*Department of Mechanical and Materials Engineering*
*University of Western Ontario*
*London, Canada*

*Brian E. Thompson and Qijun Yu*
*Foam Application Technologies, Inc.*
*Mayaguez, Puerto Rico*

*DOE Materials Technologies Team Leader: Jerry Gibbs*
*(202) 586-1182; fax: (202) 586-1600; e-mail: jerry.gibbs@ee.doe.gov*
*ORNL Technical Advisor: David P. Stinton*
*(865) 574-4556; fax: (865) 241-0411; e-mail: stintondp@ornl.gov*

---

*Contractor: Oak Ridge National Laboratory, Oak Ridge, Tennessee*
*Prime Contract No.: DE-AC05-00OR22725*

---

## Objective

- Collaborate with an automotive partner to develop an optimized heat exchanger/heat sink design that best utilizes the heat transfer properties of graphite foam to significantly reduce the size and weight of the thermal management system.

## Approach

- Study fundamental mechanisms of heat transfer in graphite foam and develop an engineering model that can be used to design and/or evaluate optimized thermal management systems using graphite foam.
- Study the boiling heat transfer on the surface of graphite foam and evaluate the performance of graphite foams as a heat spreader in such a system.
- Document the heat transfer coefficients and pressure drops of graphite foams having different structures or morphologies.

## Accomplishments

- Produced graphite foams with varying structure/morphology and demonstrated that more open structures produced improved heat transfer.

- In collaboration with General Motors (GM) and the University of Michigan, demonstrated an increase in boiling heat transfer from a foam surface by the addition of nanoparticles.
- Determined that boiling heat transfer was the best mechanism to capitalize on the heat transfer properties of graphite foam.

### Future Direction

- Collaborate with ThermalCentric and Koppers to design and build a prototype heat exchanger for evaluation by a partner from the automotive industry.
- Evaluate the performance of graphite foam as a heat spreader.

---

## Introduction

Porous graphite foam developed at Oak Ridge National Laboratory (ORNL)[1,2] is being investigated as a material to improve both single-phase and multiphase heat transfer. Graphite foam has a high effective conductivity (40–160 W/m K) because of the high material conductivity of the graphite material (800–1900 W/m K). In comparison, similar porous aluminum foams have effective conductivities of 2–26 W/m K, resulting from material conductivities of only 140–237 W/m K (for various aluminum alloys).[3] The high effective conductivity of the porous graphite foam combined with the open, interconnected pore structure facilitates high internal heat transfer and the potential for high convective heat transfer enhancement.

Work continued in FY 2006 to characterize the hydrodynamic and thermodynamic performance of graphite foam and how it impacts the development of modern heat exchangers and electronic heat sinks. Experiments were conducted in conjunction with modeling in order to explore the use of porous graphite foam for the removal of heat from power electronics.

A modified thermosyphon test rig was designed and built for the evaluation of the performance of graphite foam in these types of cooling systems. Additionally, the effect of using nanofluids on the performance of the graphite foam-based thermosyphon is being studied.

## Experimental and Modeling Study

Characterization of the hydrodynamic and thermodynamic performance of a variety of ORNL-produced graphite foams, a commercial POCO™ foam, and a couple of experimental Koppers foams was completed. The experiments were conducted on a small-scale test rig to measure the heat transfer and pressure drop across blocks of porous graphite foam. The test setup shown in Figure 1 consists of a channel with a fluid inlet and outlet; a heating element; and instrumentation to measure the flow rate, the heat input, and the fluid pressure drop across the foam block (from position 1 to 2). Graphite foam samples of different porosities and pore diameters were subjected to a range of flow rates and power densities to quantify variations in pressure drop and thermal effectiveness in the foam structure (characterized by porosity, ε, and void diameter, Dp). The flow Reynolds number (defined as $Re=\rho VpbDep/\mu$, where $\rho$ is the density of the fluid, *Vpb* is the channel bulk velocity, *Dep* is the equivalent solid particle diameter of the foam and $\mu$ is the dynamic viscosity of the fluid) was also determined.

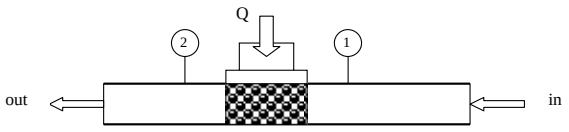


**Figure 1.** Schematic of experimental setup showing the position of the graphite foam, the fluid inlet (in) and outlet (out), and the heat input (Q).

The goal was to study the heat transfer and pressure drop obtained when passing fluid through the internal structure of the foams. Expressions describing the pressure drop and pore-level heat transfer could then be developed for use in the design of electronic heat sinks.

Table 1 lists the geometric properties and effective thermal conductivities of representative graphite foam specimens. Results were also compared with similar results for aluminum foams.

**Table 1.** Summary of properties for a selected set of graphite foam specimens tested

| Specimen | Porosity (%) | Average pore diameter (μm) | $k_{eff}$ (W/m K) |
|---|---|---|---|
| ORNL-A | 88 | 400 | 61 |
| ORNL-B | 86 | 350 | 72 |
| POCO™ | 82 | 500 | 120 |
| Koppers-A | 78 | 500 | 46 |
| Koppers-B | 92 | 850 | NA |

* As obtained from the unit-cube geometry model.

In the foams studied, the sizes of the cell windows connecting the pores varied significantly. The cell windows provide the interconnectivity between the voids and thus afford access to the internal surface area of the foam. To facilitate heat transfer, it is best to have small cell windows to maximize the internal surface area available for convection; however, small cell windows will lead to much higher pressure drops due to the hydrodynamic loss associated with rapid contraction/expansion through the cell windows. Thus, the most *open* foam will undoubtedly yield the lowest pressure, but it may not necessarily yield the highest convective heat transfer because of its lower internal surface area.

Results for the pressure drop as a function of the average channel velocity, *v*, are shown in Figure 2 for several foams of varying pore structures. The permeability and form drag coefficients established from the experiments are listed in Table 2. It is clear from Figure 2 and Table 2 that the permeability and related pressure drop differ significantly for the specimens tested, with ORNL-B having the highest fluid pressure drop and Koppers-B having the lowest. As suggested previously, the pressure drop is strongly affected by the pore diameter and, perhaps more important, the sizes of the cell windows connecting the pores. It is difficult, however, to assess the impact of pore diameter and cell window size independently based on current data. Figure 3 shows SEM images of three representative specimens.

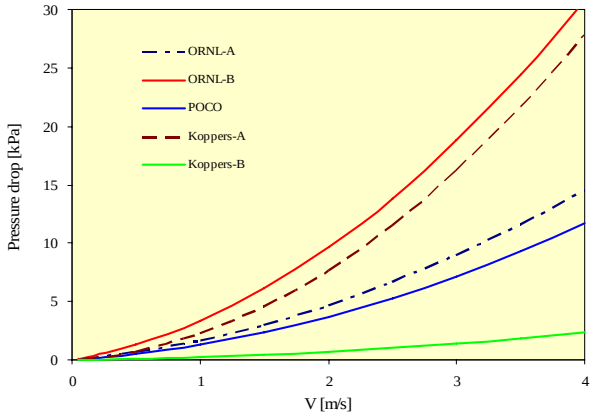


**Figure 2.** Pressure drop as a function of channel velocity, *v*. The symbols are measured data and the curves are generated from classical Darcy-Forchheimer law with the values of permeability and form drag summarized in Table 2.

**Table 2.** Summary of permeability and Forchheimer coefficients for the carbon foam specimens tested

| Specimen | Permeability, K [$m^2$] | Forchheimer Coefficient, $e_f$ |
|---|---|---|
| ORNL-A | 4.46E-10 | 0.4548 |
| ORNL-B | 2.41E-10 | 0.7444 |
| POCO™ | 6.13E-10 | 0.4457 |
| Koppers-A | 5.69E-10 | 1.3445 |
| Koppers-B | 3.89E-09 | 0.2453 |

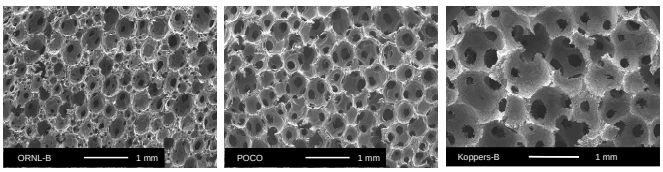


**Figure 3.** SEM images of graphite foams with varying pore structures.

Pressure drop data can be compared in terms of permeability with similar results obtained for aluminum foams. Boomsma and Poulikakos[4] evaluated the permeability of 6101 aluminum alloy foams with and without compression. The uncompressed foam had porosities in the range of 92–93% and internal surface areas of 820—2700 $m^2/m^3$, while the compressed foams had porosities in the range of 66–88% and internal areas 2 to 4 times higher. Compared with the Koppers-B foam, which has the lowest

pressure drop among the foams tested, a 6101 compressed aluminum foam of similar porosity has a permeability approximately three times higher. It is much easier to pass a fluid through the aluminum foam, largely because of the difference between the internal structures of the aluminum and graphite foams. The aluminum foam is composed of thin fused strands and large open cell windows but relatively little internal surface area. The graphite foam is composed of spherical voids and smaller cell windows but a larger amount of internal surface area. Since the low permeability of the current graphite foam is due to the restrictive cell windows that link the spherical voids, modification of the graphite foaming process could provide larger and smoother cell windows and lower the hydraulic loss.

The thermal performance of each foam was determined based on the temperature rise of the fluid across the specimen, and a thermal model that considers the block to be an extended surface heated from one side was used. The thermal performance of graphite foam was considerably better than that of an equivalent aluminum (or other metal foam) block as a result of the higher effective conductivity and the increased surface-area-to-volume ratio of the porous graphite foam. Results indicated significant advantages to using graphite foam as an extended surface convective enhancement material in energy exchange and electronic cooling applications.

## Thermosyphon System

A third-generation thermosyphon test rig was designed and built to continue the evaluation of graphite foams in an evaporative cooling system. A thermosyphon uses the latent heat of vaporization of a low-boiling-point fluid to dissipate heat. The heat is transferred from the source to the graphite foam, which is submerged in the fluid. The foam provides larger surface area and nucleation sites for boiling to occur. The vapor formed rises into the condenser section of the system, where it is condensed and drips back down to the evaporator section. This forms a closed-loop system that allows the heat to be transferred from a small source to a larger area where condensation takes place. A schematic and a photo of the thermosyphon system built for the current project are shown in Figures 4 and 5, respectively.

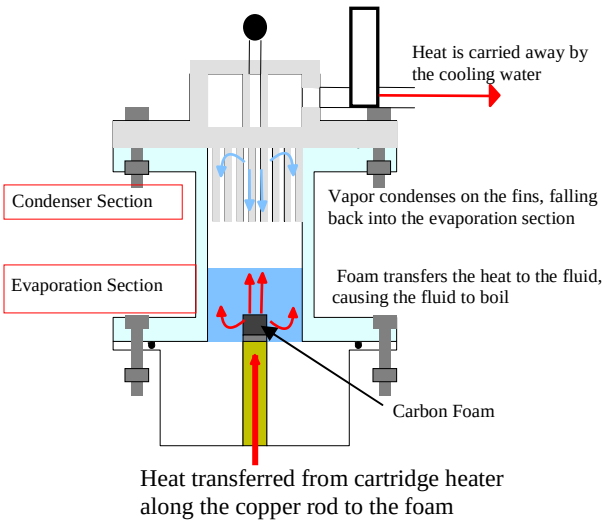


**Figure 4.** Schematic of thermosyphon test rig.

**Figure 5.** Photograph of third-generation thermosyphon test rig.

A generic heat source was created by using a cartridge heater embedded in a copper rod that was insulated in a low-conductivity glass-wool–filled PTFE housing. The heat was transferred axially along the copper rod and measured along the rod at three different locations. This allowed the heat flux to be calculated and the surface temperature of the rod to be extrapolated. The graphite foam was attached to the copper by spray-coating the bottom surface of the foam with copper and then soldering

the two surfaces together. The condenser had the top surface of its aluminum fins controlled by cooling water. The fluid used in the experiments was HFE-7000, a Novec Engineered fluid by 3M with a boiling point of 34°C.

Heat sources of three different diameters (½, ¾, and 1 in.) were used to evaluate the effect of sample size (diameter and height) on system performance. Table 3 lists the dimensions of the graphite foam samples used in the experiments, as well as their corresponding external surface areas and volumes (not accounting for the internal surface area due to the pores). Results from these tests are being used to determine if changes in the boiling convection are due to the increased surface area of the foam or to capillarity due to the internal pore structure. Samples from the first set of tests (tests 1–3) had a total external surface area of about 2.56 in.$^2$, while samples from tests 4–6 had a surface area of 1.64 in$^2$.

Figure 6 plots the heat flux versus wall temperature for samples 1–6. It was observed that samples of 0.75–in. diameter performed slightly better than samples of either 0.5- or 1-in. diameter. The reason for this improved performance is not known yet, but there may be an optimum diameter that balances the capillarity of the internal pores and the increased surface area. It was also observed that most of the nucleation sites were near the bottom of the foam.

**Addition of Nanofluid to the Thermosyphon**

In collaboration with GM, the use of nanofluids in the graphite foam-based thermosyphon was evaluated. The thermosyphon test setup was used to compare the boiling performance of pure deionized (DI) water and that of a nanofluid. The nanofluid was synthesized using 1% volume fraction of 30-nm $Al_2O_3$ particles dispersed in DI water. A photo of the nanofluid in the chamber is shown in Figure 7. Figure 8 compares the performance of the thermosyphon (heat flux versus wall temperature) using DI water with its performance using the nanofluid. It is observed that, for a given heat flux, the use of the nanofluid resulted in a lower surface temperature, indicating an increase in performance. Some nanoparticles fell out of solution and attached to the foam surface and pores. This observation is similar to those in other studies where researchers found changes in surface roughness due to sedimentation. This phenomenon may increase the surface area of the foam, provide more nucleation sites, and subsequently increase the boiling performance.

**Table 3.** Dimensions of samples used for testing.

| Test | Diameter (in.) | Length (in.) | Surface Area (in.$^2$) | Volume (in.$^3$) | SA/V |
|---|---|---|---|---|---|
| 1 | 0.960 | 0.605 | 2.548 | 0.438 | 5.820 |
| 2 | 0.710 | 0.970 | 2.560 | 0.384 | 6.665 |
| 3 | 0.475 | 1.600 | 2.565 | 0.284 | 9.046 |
| 4 | 0.960 | 0.304 | 1.641 | 0.220 | 7.456 |
| 5 | 0.710 | 0.553 | 1.629 | 0.219 | 7.442 |
| 6 | 0.475 | 0.980 | 1.640 | 0.174 | 9.441 |

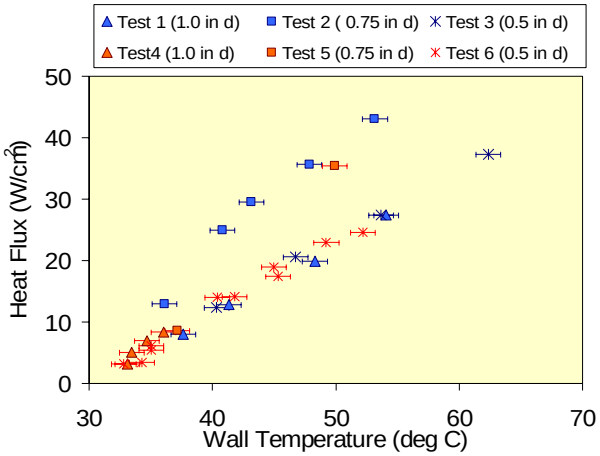


**Figure 6.** Plot of heat flux versus wall temperature for samples tested.

## Summary

Work in FY 2006 focused on developing foams with varying pore structures and morphologies and studying their hydrodynamic and thermodynamic performance. Experimental results showed a wide range of performance corresponding with the wide range of pore structures. The new ORNL and Koppers foams had the best hydrodynamic performance, i.e., lower pressure drop for a given fluid velocity. Results also showed that the thermal performance of graphite foam was considerably better than that of an equivalent aluminum foam block, indicating significant advantages for using graphite foam as an extended surface convective enhancement material in electronic cooling applications.

Studies of the boiling heat transfer on the surface of graphite foam showed that the addition of nanoparticles to the circulating fluid increases the

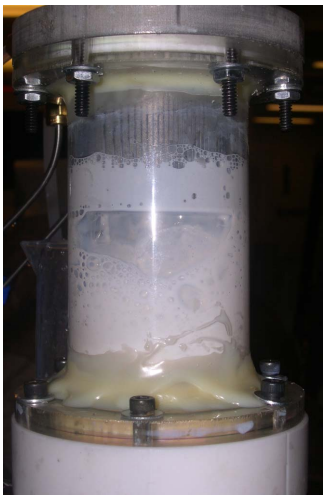

**Figure 7.** A picture of the fluid in the chamber.

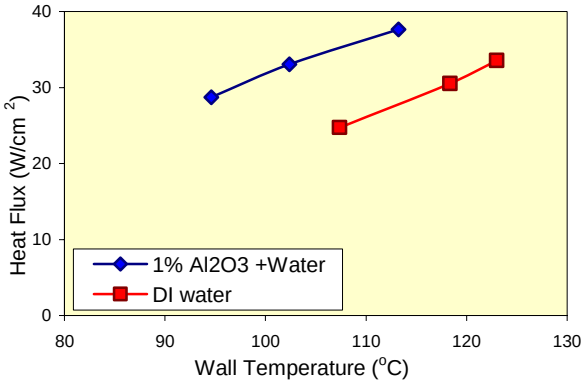


**Figure 8.** A plot of heat flux into the system and the surface temperature.

performance of the thermosyphon system. This work was conducted in collaboration with GM.

## References

1. W. J. Klett, R. Hardy, E. Romine, C. Walls, T. Burchell, "High-thermal-conductivity, Mesophase-pitch-derived Carbon Foam: Effect of Precursor on Structure and Properties," *Carbon* **38**, 953–973 (2000).
2. N. C. Gallego and W. J. Klett, "Carbon Foams for Thermal Management," *Carbon* **41**, 1461–1466 (2003).
3. W. J. Paek, H. B. Kang, Y. S. Kim, and M. J. Hyum, "Effective Thermal Conductivity and Permeability of Aluminum Foam Materials," *Int. J. of Thermophysics* **21**(2), 453–464 (2000).
4. K. Boomsma and D. Poulikakos, "The Effects of Compression and Pore Size Variations on the Liquid Flow Characteristics in Metal Foams," *ASME J. Fluids Engineering* **124**, 263–272 (2002).

## Publications/Presentations

### Publications

Q. Yu, A. G. Straatman, and B. E. Thompson, "Carbon-foam Finned Tubes in Air–water Heat Exchangers," *Applied Thermal Engineering* **26,** 131–143 (2006).

Q. Yu, B. E. Thompson, and A. G. Straatman, "A Unit Cube-based Model for Heat Transfer and Fluid Flow in Porous Carbon Foam," *ASME Journal of Heat Transfer* **128,** 352–360 (2006).

A. G. Straatman, N. C. Gallego, B. E. Thomson, and H. Hangan, "Thermal Characterization of Porous Carbon Foam—Convection in Parallel Flow," *International Journal of Heat and Mass Transfer* **49,** 1991–1998 (2006).

A. G. Straatman, N. C. Gallego, Q. Yu, and B. E. Thompson, "Forced Convection in Porous Carbon Foam," Submitted to *ASME J. Heat Transfer*, January 2006.

A. G. Straatman, N. C. Gallego, Q. Yu, and B. E. Thompson, "Characterization of Porous Carbon Foam as a Material for Compact Recuperators," Accepted in *ASME J. of Engineering for Gas Turbines and Power*, June 2006.

### Presentations

L. J. Betchen and A. G. Straatman, "An Investigation on the Effects of Porosity Gradient on Non-equilibrium Heat Transfer in Porous Carbon Foam," *Proceedings of the 14th Annual Conference of the CFD Society of Canada*, Kingston, Canada, July 2006.

A. G. Straatman, N. C. Gallego, Q. Yu, and B. E. Thompson, "Characterization of Porous Carbon Foam as a Material for Compact Recuperators," *Proceedings of the ASME Turbo Expo 2006*, Barcelona, Spain, May 2006.